

Change in ice lens formation for saline and non-saline Devon silt as a function of temperature and pressure

L. U. Arenson, D. Xia, D. C. Segó and K. W. Biggar

Department of Civil & Environmental Engineering, University of Alberta, 3-133 Markin/CNRL Natural Resources Eng. Facility, Edmonton, AB, T6G 2W2; PH (780) 492-0200; FAX (780) 492-8198; email: lukas.arenson@ualberta.ca

Abstract

During the freezing of a fine grained soil, ice lens formation changes the structure of the soil and results in frost heave. The formation of the ice lenses is very complex and dynamic. The results are presented from laboratory freezing tests on saturated Devon silt, a frost-susceptible soil. A variety of pore-water salinities, vertical pressures, and temperature gradients were used to investigate the different effects on the freezing process and the formation of the ice lenses. Using a novel experimental methodology, ice lens growth at the pore scale was observed. Fluorescein was dissolved in the pore water, which allowed to locate unfrozen water under UV light. In this manner it was possible to visually observe and measure the ice lens growth ahead of and behind the frozen fringe. It is visually shown that the thickness of the ice lenses, the distances between the ice lenses and the thickness of the frozen fringe change with changing temperature gradient, vertical pressure and salinity. In addition, the ice structure within the saline soils became more three dimensional and irregular compared to the non-saline samples, where the ice lenses develop over the entire cross section of the sample.

Introduction

Saturated fine grained soils exposed to freezing change their structure as ice lenses form. The generation of these segregated ice lenses is associated with water migration within the partially frozen soil as well as the unfrozen layers adjacent to it. The formation of ice lenses, which grow perpendicular to the thermal gradient, causes significant changes in the soil structure (e.g. Konrad and Morgenstern 1980) and hence alterations in the mechanical behavior. The behavior of frost-susceptible soils has been investigated for a long time demonstrating that grain size distribution, mineralogy, availability and salinity of the pore water, overburden pressure, and heat extraction rates have various influences (Taber 1929; Beskow 1935; Penner 1959; Williams 1967a; Williams 1967b; Anderson and Tice 1972; Konrad and Morgenstern 1982; Konrad 1987; Konrad 1990).

Water migration within the partially frozen soil is stimulated by a temperature gradient (Oliphant et al. 1983) provoking suction. Due to this suction, the warmest ice

lens forms at a certain distance behind the pore freezing front, which is at zero degrees Celsius for non-saline soils. This zone is called the frozen fringe (Miller 1972) and the temperature at which the warmest ice lens forms is known as the segregation freezing temperature (e.g. Konrad 1994). Generally, water migrates from the unfrozen zones through the frozen fringe to the warmest ice lens. Depending on the availability of water, the thickness of the final ice lens that develops under steady state thermal conditions can be significant, causing frost heave. In addition, studies have shown, that the frost heave potential decreases as the pore fluid salinity and the applied pressure increases (Konrad 1990). The temperature further influences the freezing process because solute rejection is a function of the cooling rate, dT_f/dt , at the freezing front defined by:

$$dT_f/dt = \text{Grad } T \cdot dX/dt, \quad (1)$$

where Grad T is the temperature gradient near the frost front and dX/dt the rate of frost advance.

Konrad and McCammon (1990) showed that at cooling rates below 0.1°C/day more than 90% of the solutes are rejected from the pore ice and that at rates above 3°C/day no rejection occurs. These thresholds have a significant influence when predicting the migration of contaminants in cold regions.

This paper presents the latest results of a research program that focuses on the freezing processes of frost susceptible Devon silt (Arenson et al. 2005; Xia et al. 2005). One-dimensional step freezing tests were carried out during which the formation and growth of the ice lenses was visually monitored using time-lapse photography and a special fluorescent tracer (Arenson and Segó 2006). Tests were performed at different temperature boundary conditions to study the effect of cooling rates, salinities and axial pressures. Moisture content and salinity redistributions were measured at the end of each test.

Material and Methods

A total of twelve one-dimensional step-freezing tests with access to water at the bottom (open system freezing) were carried out using Devon silt. This frost susceptible soil has a liquid limit of 32%, a plastic limit of 20%, and a specific gravity of 2.65. Initially, a slurry was prepared and deaerated using dry silt, distilled water with 5 g/L fluorescein and salts (NaCl), if applicable. The sample was consolidated under the same ambient temperature as used for the freezing stage. After consolidation the samples had a diameter of 100 mm and a height of approximately 120 mm. Details on the material, sample preparation and test equipment (Fig. 1) can also be found in Arenson *et al.* (2005) and Xia *et al.* (2005).

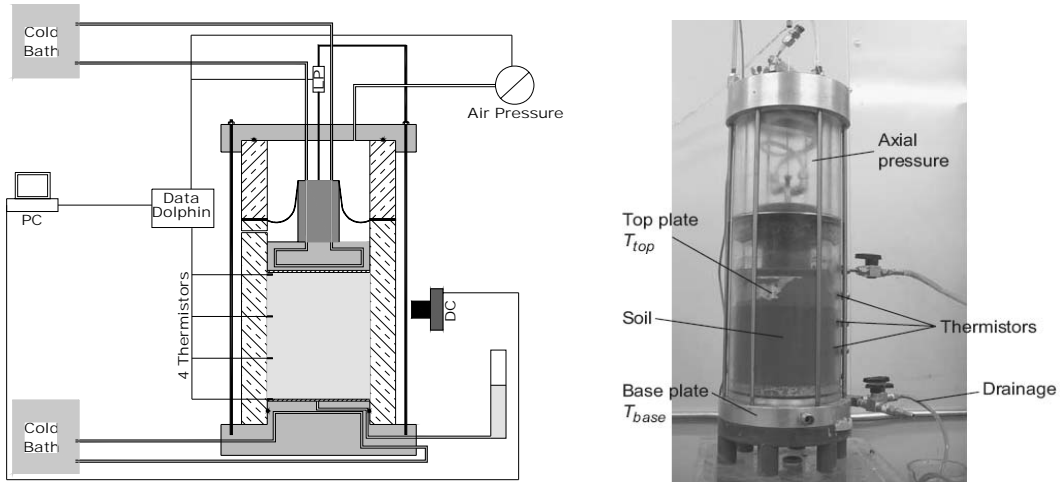


Figure 1. One-dimensional freezing cell.

Test No.	Temperatures		Salinity S (g/L)	Axial pressure	
	top (°C)	bottom (°C)		σ_c (kPa)	σ_f (kPa)
1	-5	2	0	100	0
2	-2	2	0	100	0
3	-14.5	2	0	100	0
4	-5	2	0	100	100
5	-5	2	0	200	200
6	-5	2	0	400	400
7	-5	2	5.9	100	0
8	-5	2	10.2	100	0
9	-5	2	25.7	100	0
10	-14.5	2	23.6	100	0
11	-5	2	24.4	200	200
12	-2.5	2	24.7	100	0

σ_c : consolidation pressure

σ_f : vertical pressure during freezing

Table 1. Test overview.

Table 1 summarizes the boundary conditions of the twelve freezing tests. Test No. 1 was used as a reference test. Only the top temperature was varied to change the thermal gradient and the cooling rate. The bottom temperature was kept constant at +2°C.

At the end of each freezing test, moisture contents and salinities were measured every 5 mm along the height of the sample. An electrical conductivity meter was used to measure salinities.

Results

Initial results and time-lapse photographs of the freezing processes are described in detail by Xia *et al.* (2005). The thickness of the ice lenses increased and the distance between the ice lenses decreased as the temperature gradient decreased. Similarly, ice lens thicknesses and frost heave was reduced for increased axial pressure. Changes in the frozen fringe thickness were also noted. Saline pore water resulted in a freezing

point depression and a variation in the ice lens structure within the sample. As the salinity increased the horizontal, one-dimensional ice structure changed into a three-dimensional (reticulate) structure, in which horizontal ice lenses were broken into smaller and thinner fragments. This structure enhanced water migration within the partially frozen soil. In addition, it was confirmed that at low cooling rates, solutes were rejected, which resulted in an increased salinity in the frozen fringe.

Figure 2 shows the trend in the observed frozen fringe thickness with time and height for reference test No.1. Initially, the thickness increased constantly during the fast frost penetration. After about 4 hours, the final ice lens was initiated at a sample height of 80 mm. As the cooling rates dropped at the freezing front more time is available for water to migrate toward this warmest ice lens. This resulted in an increase in the frozen fringe thickness. Later, a new lens was initiated at a lower sample height which resulted in a sudden drop in the frozen fringe thickness. These sudden jumps in fringe thickness continued until thermal steady state was nearly reached, which is at approximate 14 hours for this test. At this time the location of the frozen fringe remained unchanged and the thickness only increased slowly until it remained constant. For this test the trend in frozen fringe thickness, w_{fr} , with time, t , can be approximated with the following logarithmic relationships:

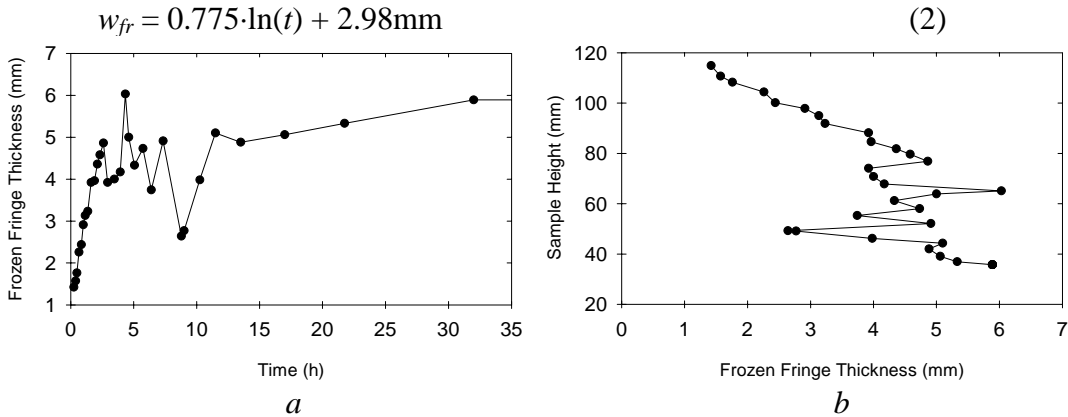


Figure 2. Frozen fringe thickness as a function of time (a) and height (b).

Not only did the final ice lens grow with time under thermal steady state, but the ice lens above it also grew concurrently (arrows in Fig. 3). Figure 4 shows the thicknesses, w_i , for both ice lenses with time, t , which could be approximated with linear functions between 20 and 82 hours.

$$w_i = 0.0129 \cdot t - 0.307 \text{ mm} \quad \text{final ice lens} \quad (3)$$

$$w_i = 0.0064 \cdot t - 0.021 \text{ mm} \quad \text{ice lens just above the final lens} \quad (4)$$

Figure 5 shows the structure of the vertical ice lenses that formed during freezing. The vertical ice lenses form quite regular pentagons with a side length of approximately 7.5 mm.

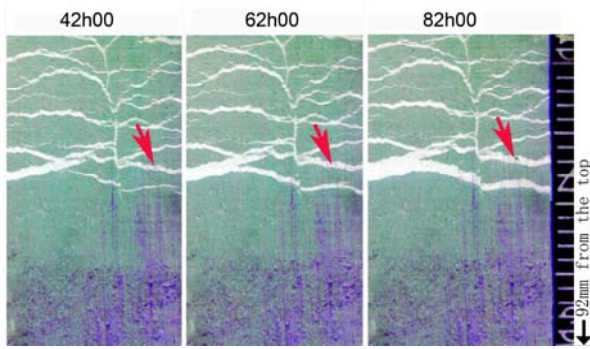


Figure 3. Growth of different ice lenses at thermal steady state.

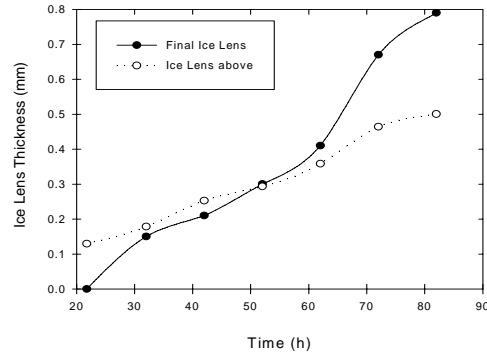


Figure 4. Change in thickness of the final ice lens and the second warmest ice lens.



Figure 5. Cross sections of the sample at the end of test No. 1. The section on the left is the frozen sample, and the section on the right the unfrozen sample.

Effect of Temperature

Three different temperatures were applied at the top of the sample (Table 1) resulting in three different temperature gradients at thermal steady state: 0.033°C/mm (Test No. 2), 0.057°C/mm (No. 1), and 0.139°C/mm (No. 3). Test No. 2 had the thickest frozen fringe whereas the other two tests showed similar behavior. Similar to Eq. 2, a logarithmic function was found to estimate the frozen fringe thickness with time:

$$w_{fr} = 1.635 \cdot \ln(t) + 4.01 \text{mm} \quad \text{No. 2} \quad (5)$$

$$w_{fr} = 1.117 \cdot \ln(t) + 1.83 \text{mm} \quad \text{No. 3} \quad (6)$$

During the initial freezing stage, cooling rates of up to 4.1°C/hour were recorded in test No. 3. This cooling rate did not allow visible ice lenses to form. The water within the voids froze without attracting additional water, i.e. the freezing happened without significant water migration. This changed as soon as the cooling rates dropped below a rate of approximately 3°C/hour (test No. 1), where thin ice lenses were already visible.

The final ice lens growth rates at thermal steady state varied between 0.013mm/hour (cf. Eq. 3) and 0.032mm/hour (test No. 2). In contrast to what would have been expected, test No. 2 showed a value that was higher than No. 1. The authors assume that this may have been because of the friction between the frozen soil and the cell wall, which will be discussed later in this paper. Because the frozen zone of test No. 2 was less thick than that of test No. 1, less friction had to be overcome, resulting in increased frost heave and final ice lens thickening rates.

Effect of Axial Pressure

Tests Nos. 1 to 6 (Table 1) were carried out using nominal vertical pressures between 0 kPa and 400 kPa. During these laboratory tests, the friction of the frozen soil on the cell walls influenced frost heave and final ice lens growth. The existence of such a friction is confirmed by the moisture content distribution after testing, which showed significant consolidation. It is assumed that consolidation of the unfrozen soil below the final ice lens not only originates from the suction at the ice lens but also from the additional resistance due to friction. The moisture content at the bottom of the sample was significantly lower than the initial one. Together with the known consolidation curve of the sample this value was used to back calculate an equivalent vertical pressure, i.e. the influence of friction. Figure 6 shows the growth rates of the final ice lens as a function of the nominal vertical stress as well as stress corrected that accounts for the friction. The corrected values were used to determine segregation potentials, which were similar to the values recorded by (Konrad and Morgenstern 1982) for comparable Devon silt.

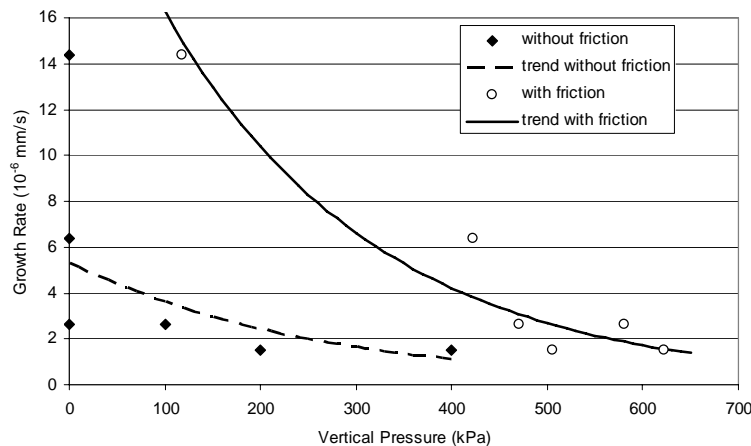


Figure 6. Growth rates of final ice lens as a function of vertical pressure.

Effect of Pore Water Salinity

The increase in pore water salinity results in a freezing point depression and therefore the pore freezing front is located at different heights for the same thermal boundary conditions. Based on the observations of the pore freezing front and the sample temperature profiles, the freezing point depression could be determined for each test

(Fig. 7). The depression measured is higher than would have been expected based on the phase diagram for NaCl ($\sim -1^\circ\text{C}$ for 20g/L). This is thought to be an effect of suction and the increased salinity in the frozen fringe. Even though the frozen fringe was located at a higher location within the sample as the salinity increased, the thickness of the frozen fringe was not affected.

As shown in Xia *et al.* (2005) at a salinity of 24 g/L, no distinct final ice lens was recorded for which a constant growth could be measured. For saline soils the growth of the final ice lens showed a bi-linear trend for saline soils with decreasing long-term growth rates as the salinity increases: 0.0058 mm/h for 5g/L, and 0.0043 mm/h for 10g/L, respectively (Fig. 8). Solute rejection might be a cause for this effect. As the saline water freezes at the bottom of the final ice lens, solutes are rejected provoking enhanced freezing point depression as well as an osmotic pressure. The osmosis reduces the solute concentration of the water via diffusion just below the ice lens. The pore water can freeze and thicken the ice lens, however, these processes slow down the ice lens growth.

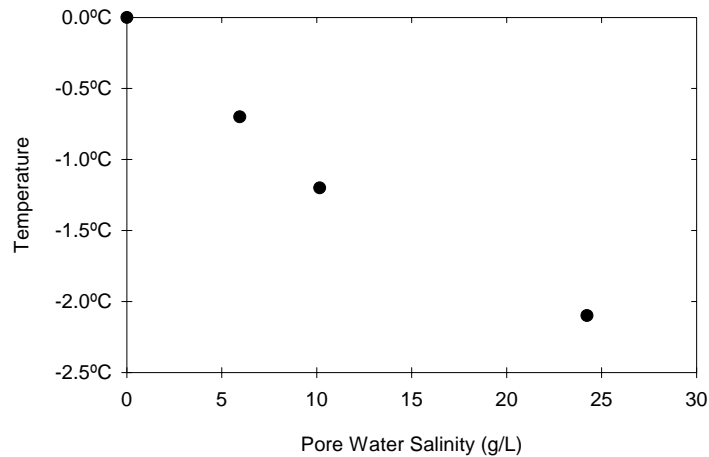


Figure 7. Pore freezing temperature as a function of the pore water salinity (NaCl).

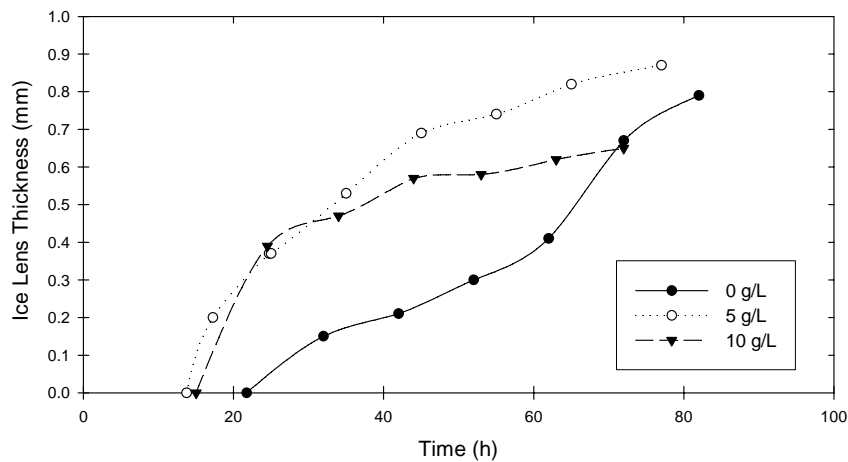


Figure 8. Final ice lens growth for different pore water salinities.

The complex dynamics during the freezing of saline pore water was confirmed by melting at the leading edge of the frozen fringe that was observed for all saline tests. After the final ice lens is formed, the freezing front should remain at a constant elevation under steady state thermal conditions. However, in all saline samples the freezing front moved up continuously at constant thermal state, i.e. part of the frozen fringe melted. This is an indicator for a locally enlarged region of freezing point depression. As the water freezes, the solute concentration increases in the soil below the ice lens, resulting in an increase in unfrozen water within the frozen fringe and hence causes melting.

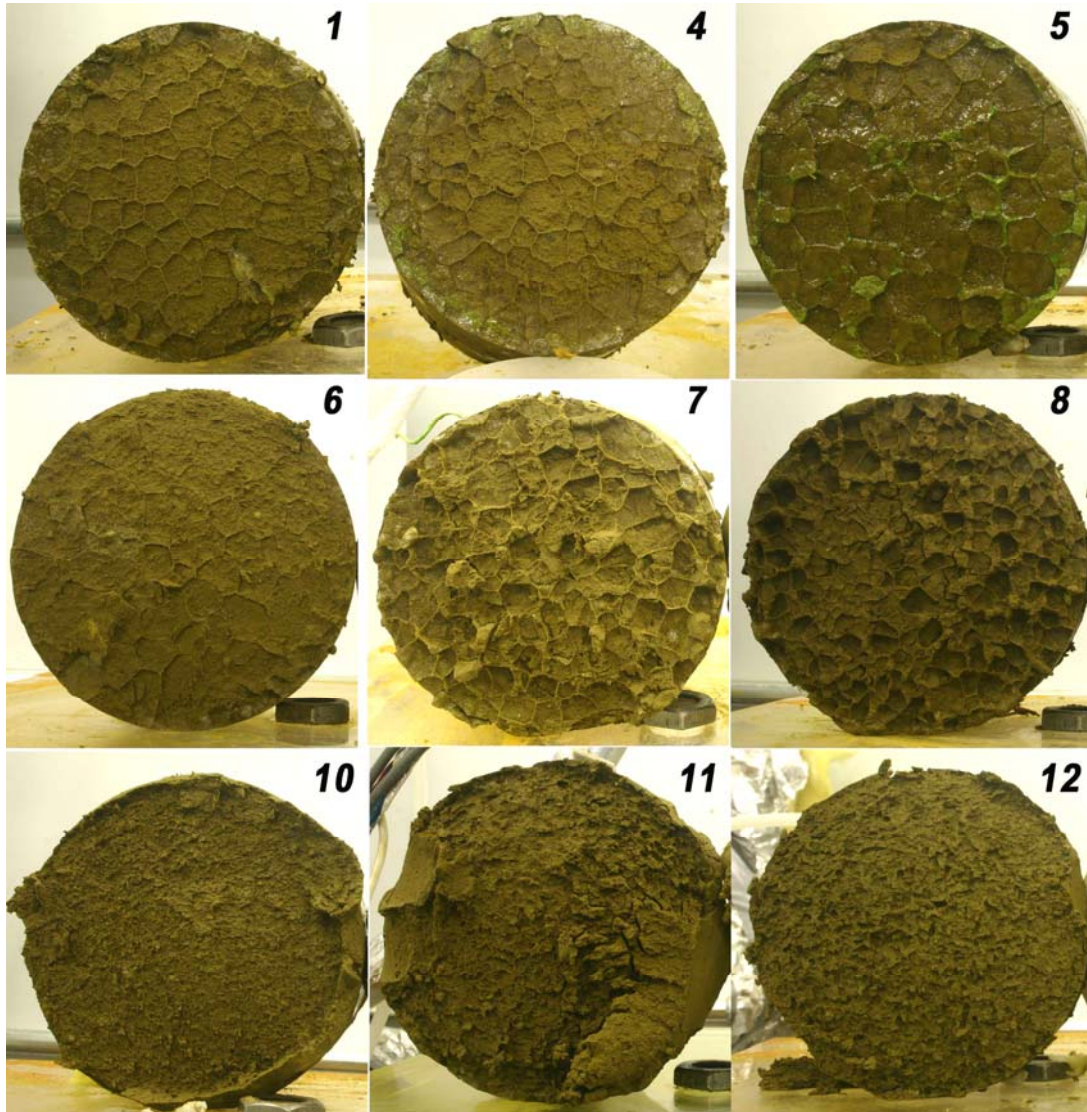


Figure 11. Cross sections for different samples after freezing.
Nos. 1,4,5,6: no salinity, No. 7: 5.9 g/L, No. 8: 10.2 g/L, Nos. 10-12: ~24 g/L.

Saline pore water provokes a significant change in the ice lens structure. The horizontal ice lenses are fragmented into smaller pieces, which results in a three-dimensional ice lens structure. Tests Nos. 1, and 4-6 were all carried out at similar temperature conditions, zero salinity, but different vertical pressures. The pentagonal pattern generated by vertical and horizontal ice lenses was very similar for all four tests (Fig. 11). As the salinity increased, the soil was less structured, and separating the samples into the frozen and unfrozen part at the end of the test was more difficult.

Conclusions

Laboratory investigations on the microstructural behavior of frost susceptible Devon silt during one-dimensional freezing showed that there are a number of dynamic processes involved during the formation of ice lenses. Temperature boundary conditions, vertical pressures and pore water salinity change the ice lens structures. As vertical pressures and cooling rates increase the ice lens thickness and the distance between the ice lenses decreases. In addition, the frozen fringe increases in thickness as the cooling rate drops. The test revealed that not only the warmest ice lens grows, but also ice lenses above (within the frozen zone) increase in thickness with time even though there is only limited access to the unfrozen zones below the pore freezing front. It is assumed that the water is drawn from the soil between the ice lenses causing localized consolidation.

The trends that were observed during these investigations revealed very interesting phenomenon that require additional analysis with new methods and under different boundary conditions. Digital image analysis might help in analyzing ice lens growth and changes in the frozen fringe. In addition, pore pressure measurements within the partially frozen soil might help with understanding the consolidation that takes place as water migrates to the ice lenses above the final one. Improvements in the cell design will assist with reducing the friction and allow unconfined ice lens growth. Miniature salinity probes can further assist in following solute rejections within the frozen fringe.

An improved understanding of the ice lens formation as a function of the cooling rate, soil type and pore water chemistry using advanced laboratory tests will help in estimating water and contaminant transport in freezing and frozen soils, and ultimately a better determination of the frozen soil characteristics.

Acknowledgements

The authors would like to thank Christine Hereygers and Steve Gamble for their assistance during the laboratory testing. The research was funded by NSERC Discovery Grants. The first author would further to acknowledge the Killam Trust as well as the Swiss National Science Foundation (grant No PA002-108947) for their financial support.

References

- Anderson, D.M. and Tice, A.R., 1972, "Predicting unfrozen water content in frozen soils from surface area measurements," *No. 393*, Highway Research Record.
- Arenson, L.U. and Sego, D.C., 2006, "The effect of salinity on the freezing of coarse grained sands." *Canadian Geotechnical Journal*, Vol. 43, No. 3, pp. 325-337.
- Arenson, L.U., Xia, D., Sego, D.C., and Biggar, K., 2005, "Brine and unfrozen water migration during the freezing of Devon silt." *Proceedings, ARCSACC*, Edmonton, AB, Canada, pp. 35-44.
- Beskow, G., 1935, "Soil freezing and frost heaving with special applications to roads and railroads." Cold Region Research and Engineering Laboratory, Special Report 91-23, pp. 41-157.
- Konrad, J.M., 1987, "The influence of heat extraction rate in freezing soils." *Cold Regions Science and Technology*, Vol. 14, No. 2, pp. 129-137.
- Konrad, J.M., 1990, "Segregation potential - pressure - salinity relationships near thermal steady-state for a clayey silt." *Canadian Geotechnical Journal*, Vol. 27, No. 2, pp. 203-215.
- Konrad, J.M., 1994, "16th Canadian geotechnical colloquium - Frost heave in soils - Concepts and engineering." *Canadian Geotechnical Journal*, Vol. 31, No. 2, pp. 223-245.
- Konrad, J.M. and McCammon, A.W., 1990, "Solute partitioning in freezing soils." *Canadian Geotechnical Journal*, Vol. 27, No. 6, pp. 726-736.
- Konrad, J.M. and Morgenstern, N.R., 1980, "A mechanistic theory of ice lens formation in fine-grained soils." *Canadian Geotechnical Journal*, Vol. 17, No. 4, pp. 473-486.
- Konrad, J.M. and Morgenstern, N.R., 1982, "Effects of applied pressure on freezing soils." *Canadian Geotechnical Journal*, Vol. 19, No. 4, pp. 494-505.
- Miller, R.D., 1972, "Freezing and heaving of saturated and unsaturated soils." *No. 393*, U.S. Highway Research Record.
- Oliphant, J.L., Tice, A.R., and Nakano, Y., 1983, "Water migration due to a temperature gradient in frozen soil." *Proceedings; 4th International Conference on Permafrost*, pp. 951-956.
- Penner, E., 1959, "The mechanism of frost heaving in soils." *Bulletin 225*, U.S. Highway Research Board.
- Taber, S., 1929, "Frost heaving." *Journal of Geology*, Vol. 37, No. 5, pp. 428-461.
- Williams, P.J., 1967a, "Suction and its effects in unfrozen water of frozen soils." *Publications of the Norwegian Geotechnical Institute*, Vol. 72, pp. 27-35.
- Williams, P.J., 1967b, "Unfrozen water in frozen soils." *Publications of the Norwegian Geotechnical Institute*, Vol. 72, pp. 37-48.
- Xia, D., Arenson, L.U., Biggar, K.W., and Sego, D.C., 2005, "Freezing process in Devon silt - using time-lapse photography." *Proceedings, 58th Canadian Geotechnical Conference*, Saskatoon, Saskatchewan. CD-ROM.